The Activity of the Neighbours of AGN and Starburst Galaxies: Towards an evolutionary sequence of AGN activity

E.Koulouridis[1,3], M.Plionis[1,2], V.Chavushyan[2], D.Dultzin[4], Y.Krongold[4], I.Georgantopoulos[1], C.Goudis[1,3]

[1]Institute of Astronomy & Astrophysics, National Observatory of Athens, I.Metaxa & B.Pavlou, P.Penteli 152 36, Athens, Greece

[2] Instituto Nacional de Astrofisica, Optica y Electronica (INAOE) Apartado Postal 51 y 216, 72000, Puebla, Pue., Mexico

[3] Physics Department, Univ. of Patras, Panepistimioupolis Patron, 26500, Patras, Greece

[4] Instituto de Astronomía, Univesidad Nacional Autónoma de México, Apartado Postal 70-264, México, D. F. 04510, México

Received _____; accepted _____

ABSTRACT

We present a follow-up study of a series of papers concerning the role of close interactions as a possible triggering mechanism of the activity of AGN and starburst (SB) galaxies. We have already studied the close ($\leq 100\ h^{-1}$kpc) and the large scale ($\leq 1\ h^{-1}$ Mpc) environment of Sy1, Sy2 and Bright IRAS galaxies and their respective control samples (Koulouridis et al.). The results led us to the conclusion that a close encounter appears capable of activating a sequence where a normal galaxy becomes first a starburst, then a Sy2 and finally a Sy1 galaxy. However since both galaxies of an interacting pair should be affected, we present here optical spectroscopy and X-ray imaging of the neighbouring galaxies around our Seyfert and BIRG galaxy samples. We find that more than 70% of all neighbouring galaxies exhibit thermal or/and nuclear activity (namely enhanced star formation, starbursting and/or AGN) and furthermore we discovered various trends regarding the type and strength of the neighbour's activity with respect to the activity of the central galaxy, the most important of which is that the neighbours of Sy2 are systematically more ionized, and their straburst is younger, than the neighbours of Sy1s. Our results not only strengthen the link between close galaxy interactions and activity but also provide more clues regarding the evolutionary sequence inferred by previous results.

Subject headings: Galaxies: Active, Galaxies: Starburst, X-ray: Galaxies, Cosmology: Large-Scale Structure of Universe

1. Introduction

Since the discovery of Active Galactic Nuclei (AGN) significant effort has been put in the attempt to reveal their nature, but we still lack a full understanding of all the aspects of activity. We are almost certain of the existence of a massive black hole (MBH) in the centre of active and even non active (Ferrarese and Merrit 2000; Gebhardt 2000) galaxies (including our own; e.g. Bozza & Mancini 2009). In active galaxies accretion of material into this BH is responsible for the excess nuclear emission that we see in the galaxy spectrum. On the other hand, the triggering mechanism and the feeding of the black hole, the structure and the physics of the accretion disk and of the torus, which is predicted by the unified scheme (Antonucci et al. 1993), the connection with star formation and the role of the AGN feedback, the origin of the jets in radio loud AGN galaxies and their influence on the IGM and ICM and even the mechanism that produces the observed IR, X-ray, and gamma-ray emission, are only partially understood. The unification model itself has not been able to fully explain all the AGN phenomenology (in particular, the role of interactions on induced activity; Koulouridis et al. 2006a,b and references therein).

The lack of detailed knowledge of key aspects of the AGN mechanism leaves us with many scattered pieces of information. Theory is unable in most cases to explain observations, and observations cannot resolve the galactic nuclei to confirm theories. Radio-loud and radio-quiet AGN, QSO type I and II, Sy1 and Sy2 galaxies, LINERs, transition galaxies between different states (TOs) and starforming galaxies, are some of the pieces we are called to unify. Examination of the properties of the host galaxies of the different types of AGN and their environment up to several hundred kpc, can give us valuable information about the central engine. In addition, the availability of large, automatically constructed, galaxy catalogues nowadays, like the SDSS, can provide the necessary statistical significance for these type of analyses. Usually the bigger the sample

the less the control we have over the spectral details of the individual galaxies and therefore the less control over the interpretation of the output results. It is dangerous to attempt to draw conclusions from analyses of large samples, that include different kind of objects, without at least having hints regarding the answers to basic questions: for example, is the Unification scheme valid for all cases of type 1 and type 2 AGN? What is the true connection between galaxy interactions, star formation and nuclear activity? What is the lifetime of these phenomena? How do LINERs fit in the general picture and are all of them AGN? Do different types imply different kind of objects, different evolutionary stages or a combination of evolution and line of sight orientation?

1.1. Triggering an AGN evolutionary sequence?

Despite observational difficulties and limitations, there have been many attempts, based on different diagnostics, to investigate the possible triggering mechanisms of nuclear activity. Most agree that the accretion of material into a MBH (Lynden-Bell 1969) is the mechanism responsible for the emission, but how does the feeding of the black hole works? There are a lot of controversial results concerning this issue. It is known and widely accepted that interactions between galaxies can drive gas and molecular clouds towards its nucleus initiating an enhanced star formation (e.g. Li et al. 2008, Ellison et al. 2008). Many also believe that the same mechanism could give birth to an active nucleus (e.g. Umemura 1998, Kawakatu et al. 2006)

Indeed, there are several studies that conclude that there is an evolutionary sequence from starburst to Seyfert galaxies (e.g. Storchi-Bergmann et al. 2001;). Furthermore, based on the number and proximity of close ($\lesssim 60 - 100\ h^{-1}$ kpc) neighbours around the different type of active (Sy1, Sy2 and BIRG) galaxies (e.g. Dultzin-Hacyan et al. 1999; Krongold et al. 2002; Koulouridis et al. 2006a,b) a very interesting evolutionary sequence has been

suggested, starting with an interaction that triggers the formation of a nuclear starburst, which then evolves to a type 2 Seyfert, and finally to a Sy1. Such connection is likely independent of luminosity, as similar trends have been proposed for LINERs (Krongold et al. 2003) and ULIRGs and Quasars (Fiore et al. 2008 and references therein). This sequence can fully explain the excess of starbursts and type 2 AGN in interacting systems, as well as the lack of type 1 AGN in compact groups of galaxies (Martinez et al. 2008).

In addition, post starburst stellar populations have been observed around AGN (Dultzin-Hacyan & Benitez 1994; Maiolino & Rieke 1995; Nelson & Whittle 1996; Hunt et al. 1997; Maiolino et al. 1997; Cid Fernandes, Storchi-Bergmann & Schmitt 1998; Boisson et al. 2000, 2004; Cid Fernandes et al. 2001, 2004, 2005) and in close proximity to the core ($\sim$50 pc), implying the continuity of these two states and a delay of 0.05-0.1 Gyr (Müller Sánchez et al. 2008) up to 0.5-0.7 Gyr (Kaviraj et al. 2008) between the onset of the starburst and the lighting up of the AGN. Davies et al.(2007), analyzing star formation in the nuclei of nine Seyfert galaxies found recent, but no longer active, starbursts which occurred 10 - 300 Myr ago. Furthermore, most of these studies (e.g. Hunt et al. 1997; Maiolino et al. 1997, Gu et al. 2001) separate type I from type II objects implying that recent star-formation is only present in type II objects. Support for the interactions-activity relation was recently provided by HI observations of Tang et al. (2008), who found that 94% of Seyfert galaxies in their sample were disturbed in contrast to their control sample (where only 19% were disturbed). We point out that a great theoretical success of the starburst/AGN connection is the quenching of the star formation induced by the AGN feedback which can explain the formation of red and dead elliptical galaxies (e.g. Springel et al. 2005a; Di matteo et al. 2005; Khalatyan et al. 2008). Recent results have found that AGN ionized outflows may carry enough energy to cease star formation in the host galaxy (Krongold et al. 2007, 2009; Chartas et al. 2008; Blustin et al. 2008). Furthermore, the correlation of morphologies of the host galaxies with the nuclear activity type can also lead

us to a possible AGN evolutionary sequence (Martínez et al. 2008).

There is also evidence pointing in the opposite direction. Li et al. (2008), analyzing SDSS data, showed that there is an increase in the starformation rate but no AGN enhancement associated to the presence of a close companion. However, they left a window open for the possibility of a delay between the onset time of the two phenomena. In any case it appears very likely that a non axi-symmetric potential, such as a tidal interaction, provides a triggering mechanism of activity.

In addition, the quenching of star formation could be due to AGN feedback, activated with a possible delay of $\sim$0.5 Gyr, inducing an evolution from a Sy2 to a Sy1 state. Should this be true, the effect of interactions on the host galaxy would not be equally observable at the different phases of the AGN evolution. Of course, such an evolutionary scenario poses some problems to the simplest version of the unified scheme.

Observations of polarized broad emission lines from type 2 AGN galaxies gave strength to the unified picture, implying that this is scattered light by the torus. However, hidden broad lines are only observable in 50% of Seyfert 2s (Tran 2003) suggesting the possible existence of true type 2 objects, i.e. objects completely lacking a BLR. The lack of a BLR can be explained in terms of a very low accretion rate (Nicastro 2000, Elitzur 2008), and/or due to even greater obscuration (Shu et al. 2008). Supporting the low accretion model, we point out that unobscured type 2 AGN galaxies have also been observed by Brightman et al. (2008) and Bianchi et al. (2008).

We stress that the evolutionary scenario does not contradict the unification scheme. It implies that different types of AGN galaxies are in fact the same object (as the unification model proposes) but not necessarily at the same evolutionary phase. However, there could be a phase where only orientation defines the appearance of a Sy1 or a Sy2 state, which is the stage where the obscuring molecular clouds form a torus but have not yet been swept

away, in agreement with the presence of polarized broad emission lines.

Taking into account the previous, when working with AGN samples, it is of crucial importance that the different types are analysed separately, in order to emphasize the similarities and the differences of each AGN type and not to smooth them by stacking them all together.

1.2. This work

This paper is the third in a series of 3-dimensional studies of the environment of active galaxies (Koulouridis et al. 2006a,b), based on previous 2D analyses (Dultzin et al. 1999, Krongold et al. 2002), and will attempt to shed some more light to the starburst/AGN connection and to the evolutionary scenario proposed in our previous papers. It is a follow-up spectroscopic study aiming at investigating the effects of interactions on the neighbours of our Seyfert and Bright IRAS galaxies.

We will discuss our galaxy samples in section §2. In §3 we present the observations and data reduction. The spectroscopic analysis and classification of the galaxies is presented in §4 and §5, while the analysis of the available X-ray observations is given in §6. Finally in sections §7 and §8 we will interpret our results and draw our conclusions. Due to the fact that all our samples are local, cosmological corrections of galaxy distances are negligible. Throughout our paper we use $H_\circ = 100\ h^{-1}$ Mpc. We use the term "active" for all galaxies that exhibit emission lines in their spectra, their origin being nuclear activity or starformation, since we believe that these two phenomena are strongly related to interactions.

2. Data

2.1. Sample Definition and Previous Results

Detailed presentation of the samples of active galaxies can be found in our previous studies (Koulouridis et al. 2006a,b). Here we only provide the basic properties of our samples and of our previous results. The original samples consisted of 72 Sy1 galaxies within redshifts $0.007 < z < 0.036$, 69 Sy2 galaxies within redshifts $0.004 < z < 0.020$ and 87 Bright IRAS galaxies within redshifts $0.008 < z < 0.018$. We also used three control samples, compiled in such a manner as to reproduce the main host-galaxy characteristics.

Using the CfA2 and SSRS galaxy catalogues we search for physical neighbours and within a projected distance $D \leq 100$ h^{-1} kpc and radial velocity separation $\delta u \leq 600$km/sec, we found (see Figure 1) that:

- The Sy1 galaxies and their control sample show a consistent (within 1σ Poisson uncertainty) fraction of objects having a close neighbour.
- There is a significantly higher fraction of Sy2 galaxies having a near neighbour, especially within $D \leq 75$ h^{-1} kpc, with respect to both their control sample and the Sy1 galaxies.
- Results based on the BIRG sample, which includes mostly starburst and Sy2 galaxies, show that an even higher fraction has a close neighbour.

In order to investigate whether fainter neighbours, than those found in the relatively shallow CFA2 and SSRS catalogues, exist around our AGN/BIRG samples, we obtained our own spectroscopic observations of all neighbours with $m_B \lessapprox 18.5$ and $D \leq 100\, h^{-1}$ kpc for a random subsample of 22 Sy1, 22 Sy2 and 24 BIRG galaxies. We found that the percentage of both Sy1 and Sy2 galaxies that have a close neighbour increases correspondingly by about

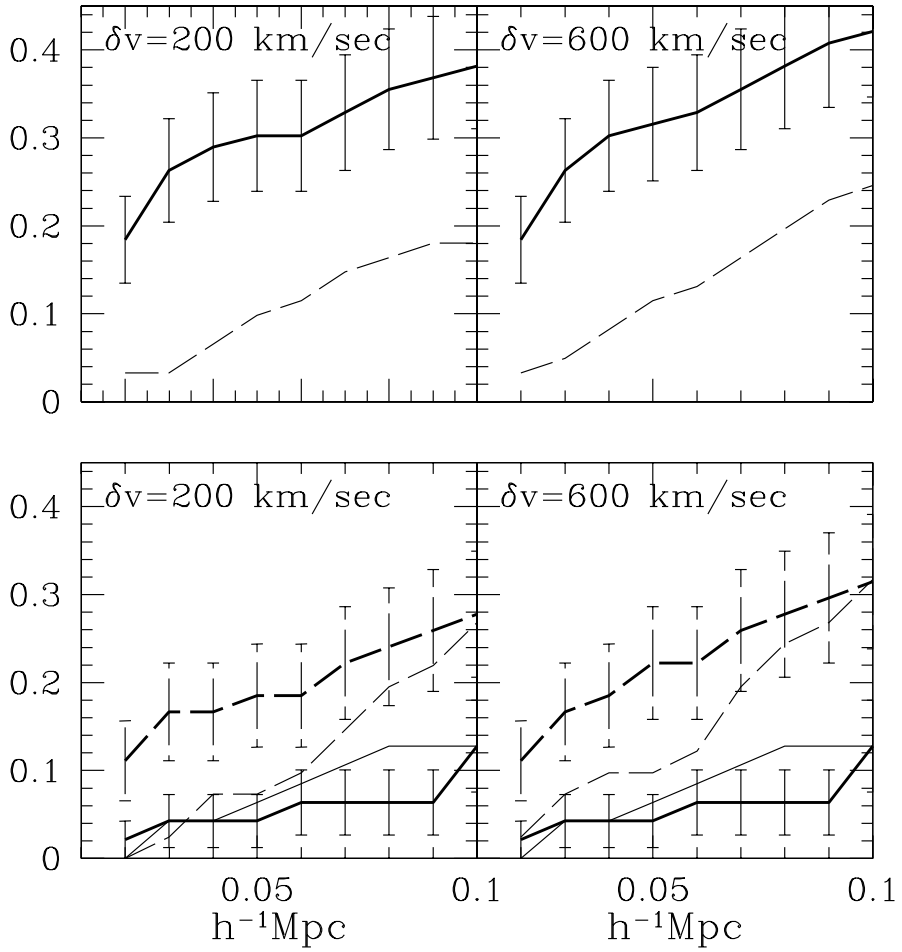

Fig. 1.— Fraction of BIRGs (top panels, thick line), Sy2s (bottom panels, thick line), Sy1s (thick dashed line) and their respective control sample galaxies (thin lines) which have their nearest neighbour within the indicated redshift separation, as a function of projected distance. Uncertainties are $\sim \pm 0.05$ in fraction (from Koulouridis et al. 2006b).

100% when we descent from $m_B \lessapprox$ 15.5 to $m_B \lessapprox$ 18.5, while the percentage of BIRGs rises only by ∼45% reaching the equivalent Sy2 levels. These results imply that the originally found difference between Sy1 and Sy2 persists even when adding fainter neighbours up to $\delta m \lessapprox$ 3, which correspond to a magnitude limit similar to the Large Magellanic Cloud.

For the purposes of the present study we compiled three samples consisting of all the neighbours around the aforementioned subsamples of Sy1, Sy2 and Bright IRAS galaxies, respectively. In Table 1, 2 and 3 we present the names, celestial coordinates, O_{maps} magnitudes [1] and redshifts of those previously mentioned Sy1, Sy2 and BIRG galaxies which have at least one close neighbour (within $\delta u <$ 600km/sec). Note that we have kept the original neighbours enumeration of the previous papers (for example, in table 3, NGC5990 has only neighbour 3, since 1 and 2 had $\delta u >$ 600km/sec). We use O_{maps} magnitudes because Zwicky magnitudes were not available for the fainter neighbours, and we needed a homogeneous magnitude system for all our objects.

2.2. Spectroscopic Observations

We have obtained spectroscopic data of all the neighbour galaxies in our samples in order to classify their type of activity. Optical spectra were taken with the Boller & Chivens spectrograph mounted on the 2.1 m telescope at the Observatorio Astronómico Nacional in San Pedro Mártir (OAN-SPM). Observations were carried out during photometric conditions. All spectra were obtained with a 2.″5 slit. The typical wavelength range was 4000-8000 Å the spectral resolution R = 8 Å. Spectrophotometric standard stars were observed every night.

[1] O (blue) POSS I plate magnitudes of the Minnesota Automated Plate Scanner (MAPS) system.

The data reduction was carried out with the IRAF[2] package following a standard procedure. Spectra were bias-subtracted and corrected with dome flat-field frames. Arc-lamp (CuHeNeAr) exposures were used for wavelength calibration. All spectra can be found at the end of the paper.

2.3. Analysis and Classification Method

In this section we present results of our spectroscopic observations of all the neighbours with $D \leq 100\ h^{-1}$ kpc and $m_{O_{maps}} \lesssim 18.5$ for all three samples of Sy1, Sy2 and Bright IRAS galaxies. We have also used SDSS spectra when available.

Our target was to measure six emission lines: H_β λ4861, H_α λ6563, [NII] λ6583, [OIII] λ5007, [SII] λ6716 and [SII] λ6731. To classify our galaxies, using the Baldwin, Phillips & Terlevich (1981, hereafter BPT) diagram, we only need four emission lines: H_β, H_α, [NII] and [OIII] (Veilleux & Osterbrock, 1987). However, it was not possible to measure the H_β and [OIII] emission lines for all of our galaxies and thus we classified many of our objects using only [NII] and H_α.

Based on the above, we adopted the following classification scheme: galaxies with no emission lines are concidered to be normal, while those with emission lines are active, meaning that they exhibit nuclear or/and enhanced starforming activity. We choose to call all starforming galaxies with prominent emission lines SB galaxies. We do not attempt to divide the starforming galaxies into more subcategories since such a categorization appears to be highly subjective and depends on the applied methodology (eg., Knapen & James,

[2]IRAF is distributed by National Optical Astronomy Observatories operated by the Association of Universities for Research in Astronomy, Inc. under cooperative agreement with the National Science Foundation.

2009).

Although we can distinguish between a SB galaxy and an AGN using only the [NII]/H_α ratio, we cannot distinguish between a low ionization (LINER) and a high ionization (Seyfert) AGN galaxy. We have also measured [OI] ($\lambda = 6300$) when possible, as an extra indicator of AGN activity. The weakness of the line, however, does not allow further use of it in a separate BPT diagram.

In Figure 2 we plot the line ratios [OIII]/H_β versus [NII]/H_α (BPT diagrams) for those neighbours of Seyfert galaxies for which we have obtained the full spectrum. We also plot the Kauffmann et al. (2003a) separation line between SB and AGN galaxies, given by:

$$\log([\mathrm{OIII}]/H_\beta) = \frac{0.61}{(\log([\mathrm{NII}]/H_\alpha) - 0.05} + 1.3 \ ,$$

and the corresponding one of Kewley et al. (2001):

$$\log([\mathrm{OIII}]/H_\beta) = \frac{0.61}{(\log([\mathrm{NII}]/H_\alpha) - 0.47} + 1.19 \ .$$

We can classify our objects in the following categories:

- SB (starburst) galaxies: all the objects which are found below the line of Kaufmann et al.
- AGN galaxies: the objects which are found above the line of Kewley et al.
- TOs (transition objects): the ones that are found between the two lines and exhibit characteristics of both an active nucleus and a starburst.

We can further separate AGN galaxies in LINERs and Seyferts based on their ionization level, namely we define LINERs as those with:

$$\log([\mathrm{OIII}]/H_\beta) < 0.90 \log([\mathrm{NII}]/H_\alpha) + 0.48$$

and the contrary for Seyferts (Schlickmann et al. *in preparation*). This division is the adaptation of the $\log([\mathrm{OIII}]/H_\beta)$ vs $\log([\mathrm{SII}]/H_\alpha)$ and $\log([\mathrm{OIII}]/H_\beta)$ vs $\log([\mathrm{OI}]/H_\alpha)$ classification lines of Kewley et al. (2006b), which separate LINERs from Seyferts.

We also classify our objects using only the $[\mathrm{NII}]/H_\alpha$ ratio, as proposed by Stasińska et al. (2006), and find that it is accurate in most of the cases (see Table 4), with only difference that it cannot distinguish between LINERs and Seyferts. Hence, we use the Stasińska et al. (2006) classification for all spectra that have no H_β region. In more detail, we classify as AGN those objects with $\log([\mathrm{NII}]/H_\alpha) > -0.1$, as SB those with $\log([\mathrm{NII}]/H_\alpha) < -0.4$, and as TO the rest.

Further classification of the Seyfert galaxies in type 1 and type 2 was obtained by direct visual examination of the spectra and the broadening of the emission lines. No Sy1 activity was discovered in any of the galaxies and therefore all neighbours classified as AGN should be considered of type 2. In Table 4 we list for all neighbours their line ratios and the two different classifications. Evidently, in most cases the classifications are absolutely consistent.

3. Results and analysis.

3.1. Activity of the neighbours.

In this section we discuss in more detail the results of our spectroscopy and classification. We can draw our first results for each sample separately inspecting Table 4. From the analysed 15 neighbours of Sy1 only 4 are normal galaxies, while 7 of them are SB galaxies, 3 are classified as TOs and one is classified as AGN. Similar results hold for the neighbours of Sy2 galaxies. 4 out of 16 neighbours do not show activity, 7 are SB galaxies, 2 TOs, 2 AGN (ambiguous classification). In both cases, Seyfert galaxies show at least 70%

of activity in their vicinity. For the Bright IRAS sample this percentage reaches almost 83% since only 4 out of 23 neighbours are inactive, 10 SB galaxies, 6 TOs and 2 AGNs. However, we should stress out that we did not find any Seyfert galaxy in our samples and even those classified as AGN, by their $NII/H\alpha$ ratio and the presense of the forbiden [OI] line, are objects of low luminosity or LINERs.

Note however that due to lack of detailed spectroscopic data for the majority of our BIRG's, it is not possible to correlate their activity type with that of their neighbours. Only a crude classification was possible in Koulouridis et al. (2006b) by cross-identifying literature classifications while also using the available SDSS data, which showed that BIRGs exhibit various activity types. Therefore we will use in the remaining study, the neighbours of only those BIRGs which have SDSS spectra and which we classified as AGN. Accordingly, we plot in figure 2 the three neighbours of two Sy2 BIRGs. A more detailed analysis of the whole BIRG sample will be subject of a future work.

One of the most interesting results of our analysis is that the neighbours of Sy2 galaxies have systematically larger values of [OIII]/H_β than the neighbours of Sy1 galaxies (see Figure 2). Since this ratio shows the ionization level and the age of the starburst (e.g. Dopita et al. 2006) we conclude that the neighbours of type 2 Seyferts tend to be more ionized than the neighbours of type 1, and their starburst is younger. The straight dashed line, in the starforming area, which separates LINERs from Seyferts ([OIII]/$H_\beta = 0.90([\mathrm{NII}]/H_\alpha) + 0.48$), clearly also separates the neighbours of Sy1s and Sy2s. All objects, classified as TOs, above this line are Sy2/Starburst composites, while beneath the line are LINER/Starburst composites.

We suggest that galaxies between the curves of Kauffmann et al. (2003a) and Kewley et al. (2001) migrate from a pure starforming phase to a pure AGN phase. This is of great importance to a possible evolutionary scenario and will be discussed further in §5.

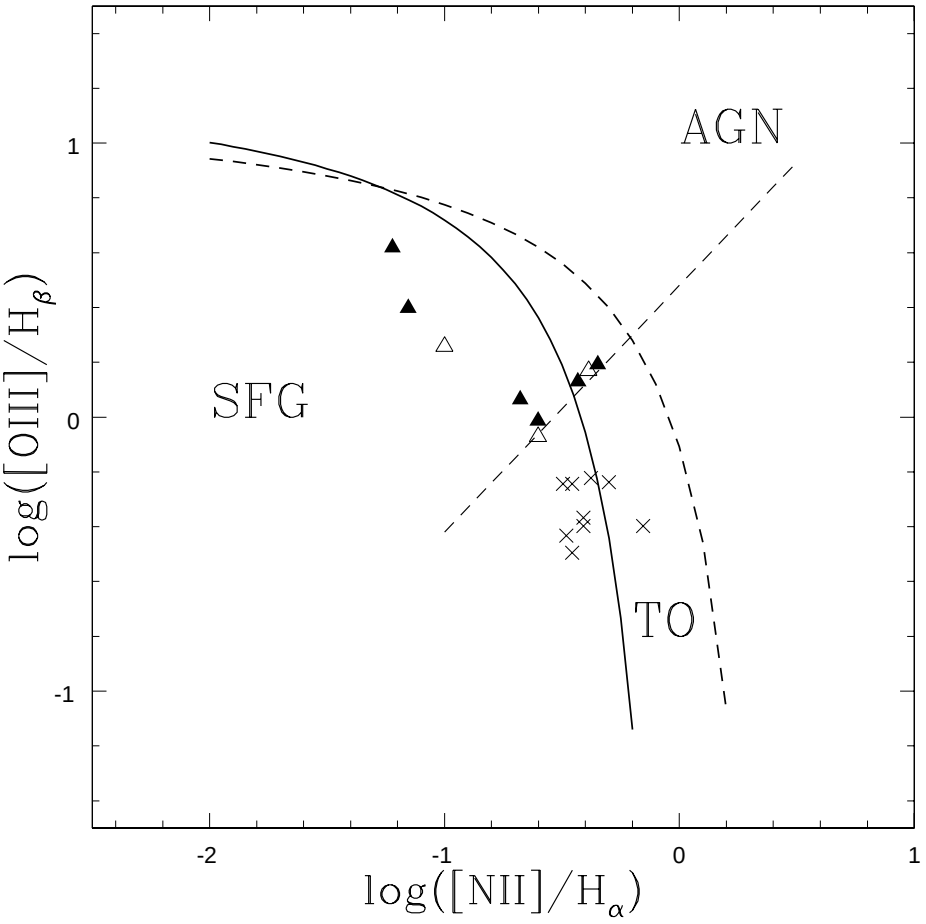

Fig. 2.— BPT classification diagram of the neighbours of Sy1 and Sy2 galaxies. The thick dashed line is the starburst-AGN demarcation, given by Kewley et al. (2001), the continuous thick line is the demarcation of Kauffmann et al. (2003a), the straight thin dashed line is the Seyfert/LINER demarcation by Schlickmann et al.(*in prep.*). The triangles are the neighbours of Sy2 galaxies (empty triangles are the neighbours of BIRG Sy2s). The crosses are the neighbours of Sy1 galaxies. Note that the neighbours which we have classified as AGN do not appear here due to lack of their spectral H_β region, as we have already mentioned in the text.

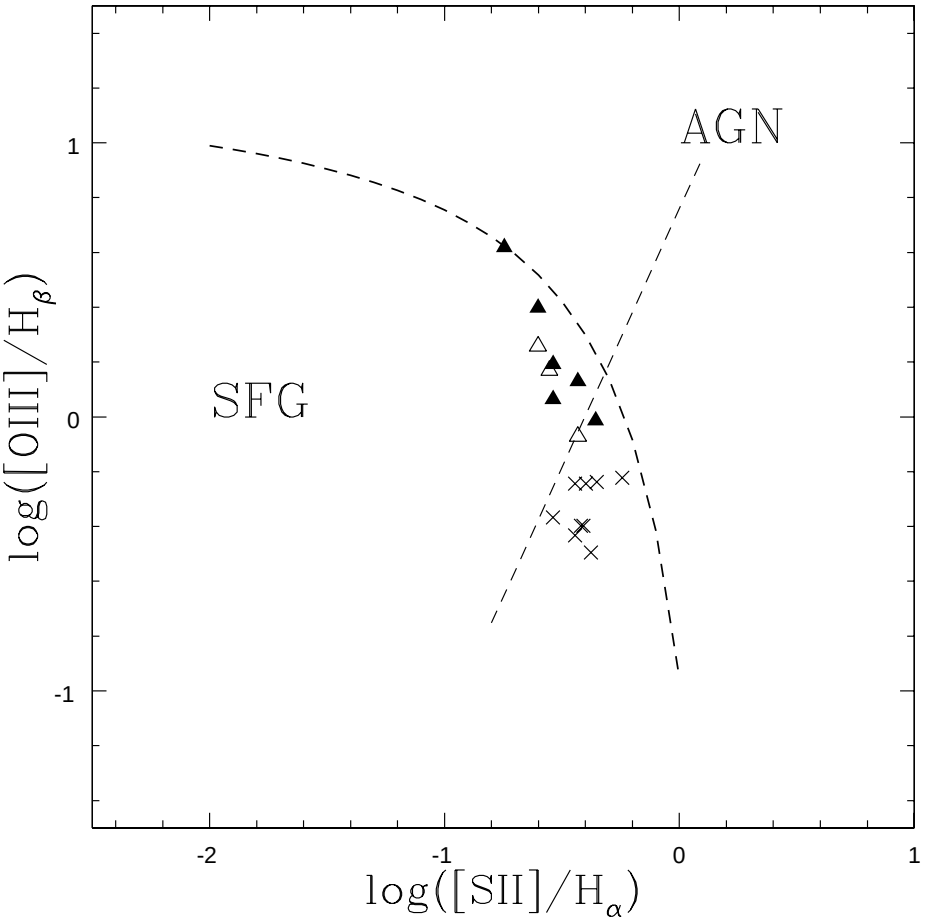

Fig. 3.— The log([OIII]/H_β) vs log([SII]/H_α) BPT classification diagram. Point types and lines are as in Figure 2.

Finally we also plot in figure 3 the [OIII]/H_β ratio vs [SII]/H_α for all the neighbours for which we could measure their [OIII]/H_β ratio[3]. Qualitatively, the same results as in Figure 2 are repeated here as well. The dividing lines are given by Kewley at al. (2006b). However, we do not have the respective line of Kauffmann et al. (2003a) and thus we cannot separate pure starburst galaxies from composite objects. Since the measurement of the [SII] doublet bears in general greater errors, we will draw our results based on the [NII] forbidden line. Nevertheless, once more, we see how close to a composite state are the neighbours of active and starburst galaxies. We should mention here that Kewley at al. (2006a) showed that the starforming members of close pairs, lie closer to the classification line than the starforming field galaxies.

Summarizing our main results of this section:

- More than 70% of the neighbours of all AGN or BIRG samples exhibit activity.
- The neighbours of Sy2s are systematically more ionized, and their starburst younger, than the neighbours of Sy1s.

It would be interesting at this point to correlate the activity type of the neighbours to other properties of the host galaxy. To this end, we analyse in the following section the relation between the magnitude and the activity properties of each central active galaxy to those of its neighbour.

[3]We have excluded a complicated object with three neighbours, out of which two are merging and unresolved (UGC7064).

3.2. Magnitude analysis

Since we have already applied a homogeneous magnitude system to our samples, we can now study whether there is a correlation between the activity of the interacting galaxies and their size. On average, size and magnitude are correlated in small redshift intervals (as it is in our case) and therefore the activity-size comparison can be performed in two ways: Either by comparing their absolute magnitudes or alternatively by examining the apparent magnitude difference of the interacting pair.

While the latter is a good tracer of the strength of the interaction, the former can possibly point out differences between intrinsically large and small galaxies. We performed both type of analyses but we did not find significant differences between them, something which should probably be attributed to the fact that our galaxies reside in the local universe ($z \lesssim 0.03$). Therefore, we present results based on the pair relative apparent magnitude difference. We define the relative size of a neighbour using the apparent magnitude difference with its central AGN, Δm, according to the following:

1. **VL** (Very Large): $\Delta m \leq 0.5$
2. **L** (Large): $0.5 \leq \Delta m \leq 1.5$
3. **S** (Small): $\Delta m \geq 1.5$

In Table 5 and figure 4 we present the results of this classification. Note that with M we mark a merging galaxy pair. Although this classification is rough and objects could lie near the limiting borders, we can still derive valuable information, as we will see below. Examining Table 5 and fig.4 it becomes evident that:

(a) small neighbours are preferentially SB galaxies,

(b) all small neighbours at distances greater than ~ 30 kpc are starbursts,

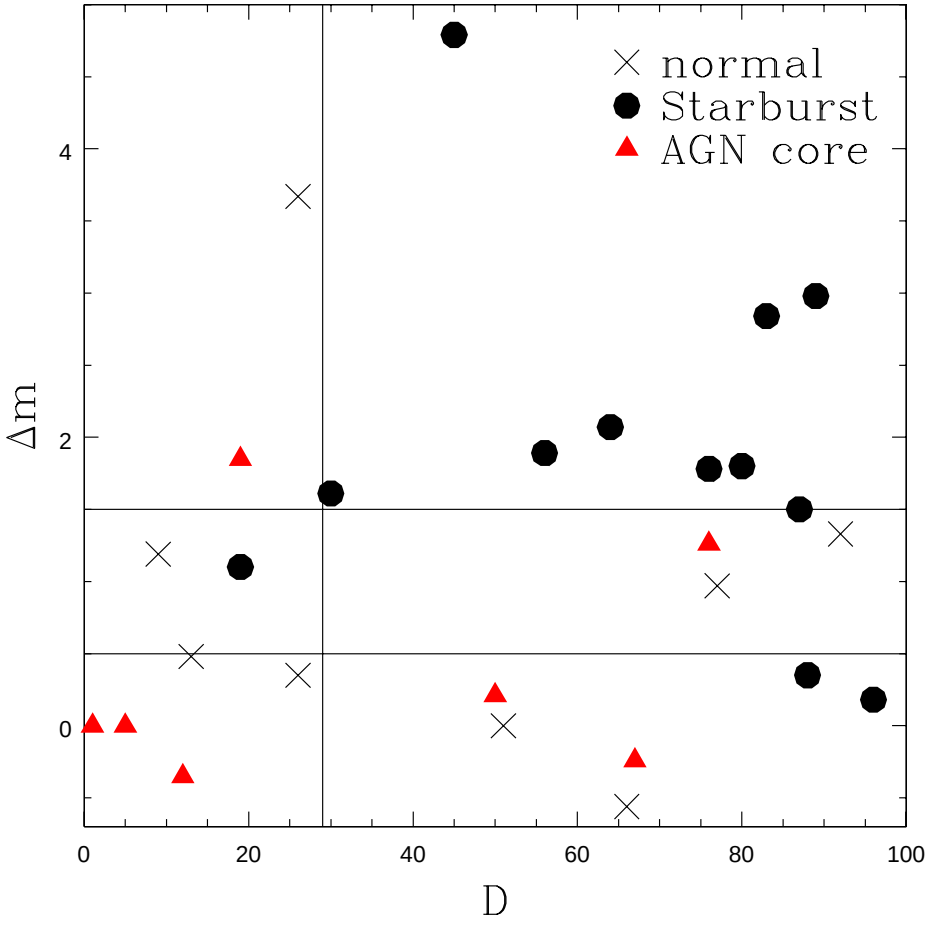

Fig. 4.— The magnitude difference Δm of the AGN-neighbour pair as a function of their relative separation D. The colour/shape coding denotes the activity type of the neighbour. For simplicity we mark all galaxies that show AGN activity and TO's with red triangles. For more details see Table 5. The horizontal lines denote the magnitude classification of the neighbours (see text), the vertical the limit $\gtrsim 30$ above which we find the great majority of SB neighbours.

(c) the large majority of starbursts are found at separations $\gtrsim 30$ kpc from the central Seyfert galaxy,

(d) all the inactive neighbours of Seyferts fall in the large or very large category,

(e) most of the neighbours which host an AGN or are transition objects, fall again in the large or very large category,

From the above we can infer that when a small galaxy is in interaction with a much larger one, the encounter leads to a starburst in the smaller companion. Therefore, although a small neighbour appears to always exhibit enhanced star-formation, induced by the interaction, it does not show any AGN activity. This could be due to the absence in small galaxies of a massive black hole (Wang, Kauffmann 2007).

If this is correct, only galaxies which experienced a major merger can exhibit AGN activity and this could be the reason why AGN hosts are more frequently found in early type galaxies (e.g. Marquez & Moles 1994; Moles, Marquez, & Perez 1995; Ho et al. 1997; Knapen et al. 2000; Wake et al. 2004). This can also account for the big number of starburst galaxies in our samples. Nevertheless, the absence of small starburst galaxies within $D \lesssim 30 h^{-1} kpc$, could imply that the interaction is so strong in such close distance that leads to the gas stripping of the small neighbour. Apparently, the interaction affects differently a large neighbour which can be found in any activity state or even remain unaffected and thus inactive. Finding relatively many massive galaxies in a normal state implies a probable delay of the outcome of the interactions or even that the interactions are not affecting those galaxies in a significant way. However, both scenarios are evenly probable since we also find many big neighbouring galaxies showing AGN activity. In the X-ray analysis section we also address this issue.

The morphology of the host galaxy, the mass of the central black hole or even more

complicated issues, like the spin of the BH or the strength of the AGN feedback, could also play a role to the viability of the starburst phase and the feeding of the black hole.

3.3. The XMM-Newton observations

In addition we have explored whether the neighbours present nuclear activity, using X-ray observations from the *XMM* public archive. We find that 13 target fields have been observed by *XMM*. However, some of them are very bright and have been observed in partial window mode rendering the observations in center of the Field-of-View unusable (NGC5548, NGC863, 1H1142-178, NGC7469). The list of the remaining observations (12 neighbours and 10 central Seyfert galaxies) is shown in table 5.

There, we present X-ray fluxes for the detections as well as upper limits for the non-detected sources. The fluxes have been taken from the 2XMM catalogue (Watson et al. 2009). The fluxes refer to the total 0.2-12 keV band for the PN detector or the combined MOS detectors in the case where PN fluxes are not available. In the 2XMM catalog, fluxes have been estimated using a photon index of $\Gamma = 1.7$ and an average Galactic column density of $N_H = 3 \times 10^{20}$ cm^{-2}. In the same table we quote the 2XMM hardness ratios derived from the 1-2 keV and 2-4.5 keV bands (hardness ratio-3 according to the 2XMM catalogue notation). The upper limits, derived using the *FLIX* software, are estimated following the method of Carrera et al. (2007). This provides upper-limits to the X-ray flux at a given point in the sky covered by *XMM* pointings. The radius used for deriving the upper limit was 20 or 30 arcsec depending on the presence of contaminating nearby sources.

In Figure 5 we present the X-ray to optical flux diagram $f_X - f_B$ (e.g. Stocke et al. 1991). The X-ray to optical flux ratio for any source is given by:

$$\log f_X/f_B = \log f_X + 0.4B + 4.54 \quad (1)$$

where f_X is the 0.2-12 keV flux and B is the Johnson B magnitude; we assumed $B-V \approx 0.8$.

This diagram provides an idea on whether a galaxy may host an active nucleus. This is because AGN have enhanced X-ray emission at a given optical magnitude relative to normal galaxies. The space usually populated by AGN is shown between the lines. Note however, that Seyfert-2 galaxies with large amounts of absorption, as is the case of NGC7743 (Akylas & Georgantopoulos 2009), lie below the lines as their X-ray flux has not been corrected for X-ray absorption. One source which lies in the AGN regime (7682-N1) can be immediately seen. This has been classified as a TO galaxy in the optical spectroscopic analysis and is the only one of the 12 neighbours (with XMM observations) having an active nucleus based on spectroscopy. Additional information on the nature of our sources can be extracted from the hardness ratios. Two sources NGC526-N2 and N1358-N2 have hardness ratios suggesting absorption $N_H \approx 10^{22}$ cm^{-2}, consistent with the presence of a moderately obscured active nucleus. Both these galaxies present no optical emission and thus classified as normal, based on their optical spectra. However, as we saw in the previous section, these galaxies fall into the category of relatively massive neighbours, many of which present AGN activity. In other words, the lack for optical emission lines from the nucleus of these objects could be a result of obscuration. In addition, we should mention here that in the group of objects with an X-ray observation, all Galaxies classified as "normal" through optical spectroscopy present an X-ray detection, indicating possibly the presence of nuclear activity. In contrast, all SB galaxies except one in the X-ray subsample do not show an X-ray detection.

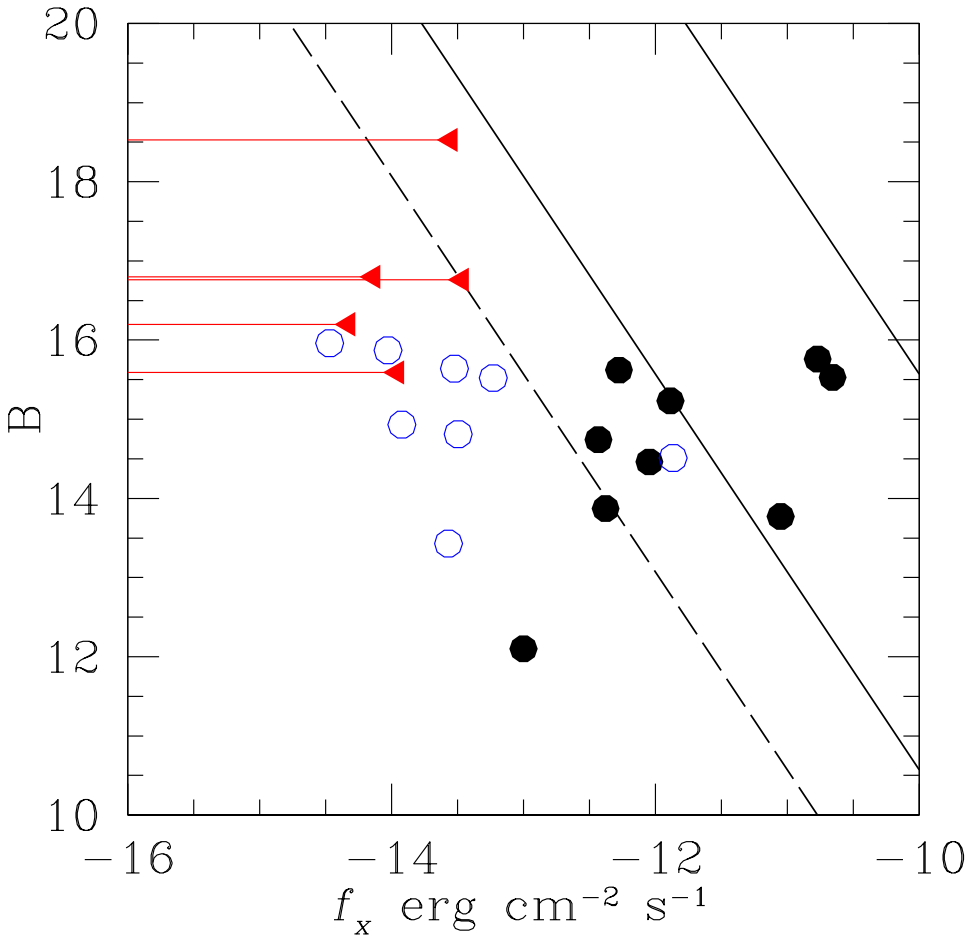

Fig. 5.— The X-ray (0.2-12 keV) to optical (B-band) flux diagram for both the AGN targets (solid circles) and the neighbors (open circles). The open triangles (upper limits) denote the neighbors with no X-ray detection. The upper, lower solid line and the dash line correspond to $f_X/f_B = +1, -1, -2$ respectively.

4. Interpretation of our results

4.1. Interacting pair: the central AGN's neighbour

We will first examine what happens to the companion galaxy of the central AGN, which we believe depend on its magnitude/size.

As we discussed earlier, interactions would drive molecular clouds to the centre of the galaxy and create a starburst. If the galaxy is small enough not to have a sufficiently massive central black hole, then there is no AGN activity nor feedback and this could possibly explain why we find most of our small neighbours in a starburst state, independently of the activity of the interacting AGN.

Our most important result is that *the star forming neighbours of Sy2 galaxies appear to be always more ionized than the ones around Sy1 galaxies and their starburst is younger.* This is a direct indication that indeed the Sy1 stage follows the Sy2 stage.

If now the neighbouring galaxy is large enough to host a central super massive black hole, it would follow the same evolutionary path as the central AGN or BIRG, which is described in the next subsection.

4.2. Interacting pair: the central AGN or BIRG.

We now attempt to fit our results in an evolutionary scenario, partly presented in a previous paper of the series (Koulouridis et al 2006b). Something that is nowadays undisputed is the role of interactions in the creation of a starburst. Molecular clouds are being forced towards the galactic center, become compressed and light up the galaxy as a starburst.

Despite the fact that the exact mechanism is still unknown, in the local universe an

accretion rate of $\sim 0.001 - 0.1 M\odot$/yr is needed to fuel the black hole. Theoretically this can only be achieved by means of a non axisymmetric perturbation which induces mass inflow. Such perturbations are provided either by bars or by interactions.

Whichever the mechanism may be, the result is the feeding of the black hole and the activation of the AGN phase, maybe $\sim 0.5 Gyr$ after the initial interaction took place. An interaction certainly predicts such a delay, since after the material has pilled up around the inner Linblad resonance, producing the Starburst, it can be chanelled towards the nucleus by loosing significant amounts of angular momentum, a process which is not instantaneous. Therefore, a delay exists between the SB and AGN phases, where active nucleus and circumnuclear starburst coexist. In this initial phase, the nucleus is heavily obscured by the still starforming molecular clouds and we can observe a transition stage of composite Sy2-starburst objects.

The most probable manner for the AGN to dominate is to eliminate the starburst, possibly by the AGN outflows or by radiation pressure. Outflows from the core have enough energy to dissipate the material around it and suffocate star formation (eg. Krongold et al. 2007, 2009, Hopkins & Elvis 2008).

This could also take some time and as the starburst fades, the Seyfert 2 state starts dominating to be followed, at the end, by a totally unobscured Sy1 state, possibly $\sim$ 1Gyr after the initial interaction.

4.3. From Sy1 back to normality

Here we will present a scenario which describes a possible avenue for a Sy1 galaxy to return to its formal normality.

Eventually, the radiation pressure can drive away not only the obscuring clouds but

also the BLR and thus the AGN is driven to a totally unobscured Sy2 phase, followed later, and as accretion keeps diminishing because of the exhaustion of accreting material, by a LINER phase. However, we should note here that a pure Sy2 (without BLR) can also exist during the initial phase of the sequence, when accretion can also be very low, though in this stage might be obscured by the material of the surounding SB.

In the case where the BLR is still present, after all obscuration is gone, it is possible not to observe the "naked" Sy2 after the Sy1, but instead a type I LINER. On the other hand, if the BLR vanishes before the obscuring material, then an unobscured Sy2 appears immediately after the obscured one, omitting the Sy1 phase. Finally, the LINER turns into a low luminosity transition object (TO) which exhibits a combination of LINER and low ionization starforming characteristics and then shuts off. We repeat that not all TOs exhibit low luminosities and, as we have mentioned ealier in §3.1, some may be in transition from a pure SB to a pure Sy2 phase following the exact opposite evolutionary path.

This scenario proposes a circular process which drives a normal interacting galaxy through starbursting and different AGN states back to normality. It is clearly not a simple model but surely a unified one. It combines previously proposed evolutionary scenarios between starbursts and Seyferts or between different types of AGNs to a single route covering all the BPT diagram. Interestingly, it predicts two totally different populations of Sy2 galaxies, one previous to and one following the Sy1 phase. The former possesses HBLR while the latter does not. However, as we have commented before, pure Sy2 galaxies can also exist in the initial phase.

However, this is not the only possible scenario. Krongold et al. (2003) concluded that type II LINER and transition LINER galaxies are more often in interaction than type I LINER galaxies. Based on this result, an alternative scenario where all galaxies evolve from normal to AGN of any luminosity was proposed. In this case all objects would return to

normal when the material driven to the center by the interaction exhausts.

From our point of view, in an ever evolving universe such schemes, as presented previously, are more probable than the original unification paradigm which proposes a rather static view of AGN. Of course, orientation could and should play a role between the obscured Sy2 and Sy1 phase, where the relaxing obscuring material forms a toroidal structure.

5. Conclusions.

We have found that the large majority ($> 70\%$) of close neighbours of AGN (being Sy1 or Sy2) and of Bright IRAS galaxies show activity, mostly starbursting but AGN as well. Furthermore, the close neighbours of Sy1 galaxies, being starbursts or AGN, are less ionised and thus seem to be a different, more evolved, population than those of Sy2s.

These results are in the same direction as those of our previous papers, ie., the significant excess of neighbours around Sy2s and BIRGs but not around Sy1s, and support an evolutionary sequence of galaxy activity, induced by interactions, the main path of which is from inactivity, starburst, Sy2, Sy1 and back to inactivity, since the "active" phase should cease with AGN feedback. Finally, such sequence could be repeated by a new encounter.

The time needed for type 1 activity to appear should be larger than the timescale for an unbound companion to escape from the close environment, or comparable to the timescale needed for an evolved merger ($\sim$ 1Gyr, see Krongold et al. 2002). If our scenario is correct, then there should be two distinct populations of Sy2s: the obscured ones which pre-exist the Sy1 phase and should exhibit close companions and the "naked" ones which appear later and should be isolated.

The results of our analysis also provide valuable guidelines for future studies of the

AGN environment, since they point out two very important issues:

[a.] Taking under consideration the possible evolutionary scheme discussed and if indeed strong interactions can be traced only until the first Sy2 phase of the phenomenon, the use of large AGN samples, without discriminating the different activity types, would introduce a large confusion to the interpretation of the results of studies of the AGN environment. For example, keeping indiscriminately the huge population of LINERs in analyses of AGN samples could result in confusion regarding the AGN local environment.

[b.] Starburst galaxies should not be handled under any circumstances as normal galaxies, since the starburst/AGN connection appears quite plausible and composite objects do exist anyway. In a nutshell, all different categories of active galaxies should be treated separately.

There are still many unresolved issues and caveats concerning these studies, since the evolutionary sequence is not unique and should also depend on the geometry, the density and other factors of the obscuring and the accreting material, as well as on the mass of the host galaxy and its black hole.

EK thanks the IUNAM and INAOE, were a major part of this work was completed, for their warm hospitality. We also thank OAGH and OAN-SPM staff for excellent assistance and technical support at the telescopes. VC acknowledges funding by CONACYT research grant 39560-F and 54480-F (México). MP acknowledges funding by the Mexican Government research grant No. CONACyT 49878-F, VC by the CONACyT research grant 54480 and DD support from grant IN100703 from DGAPA, PAPIIT, UNAM. This research has made use of the MAPS Catalog of POSS I supported by the University of Minnesota (the APS databases can be accessed at http://aps.umn.edu/) and of the USNOFS Image and Catalogue Archive operated by the United States Naval Observatory, Flagstaff Station (http://www.nofs.navy.mil/data/fchpix/). Funding for the SDSS and SDSS-II has been

provided by the Alfred P. Sloan Foundation, the Participating Institutions, the National Science Foundation, the U.S. Department of Energy, the National Aeronautics and Space Administration, the Japanese Monbukagakusho, the Max Planck Society, and the Higher Education Funding Council for England. The SDSS Web Site is http://www.sdss.org/.

REFERENCES

Akylas, A, & Georgantopoulos, I., 2009, arxiv/0904/3459

Antonucci, R. 1993, ARA&A, 31, 473

Baldwin, J. A., Phillips, M. M., & Terlevich, R. 1981, PASP, 93, 5

Bianchi, S., Corral, A., Panessa, F., Barcons, X., Matt, G., Bassani, L., Carrera, F. J., & Jiménez-Bailón, E. 2008, MNRAS, 385, 195

Boisson, C., Joly, M., Moultaka, J., Pelat, D., & Serote Roos, M. 2000, A&A, 357, 850

Boisson, C., Joly, M., Pelat, D., & Ward, M. J. 2004, A&A, 428, 373

Bozza, V., & Mancini, L. 2009, ApJ, 696, 701

Brightman, M., & Nandra, K. 2008, MNRAS, 1110

Carrera, F.J. et al., 2007, A& A, 469, 27

Chartas, G., & Saez, C. 2008, AAS/High Energy Astrophysics Division, 10, #26.09

Cid Fernandes, R. J., Storchi-Bergmann, T., & Schmitt, H. R. 1998, MNRAS, 297, 579

Cid Fernandes, R., Heckman, T., Schmitt, H., Delgado, R. M. G., & Storchi-Bergmann, T. 2001, ApJ, 558, 81

Cid Fernandes, R., Gu, Q., Melnick, J., Terlevich, E., Terlevich, R., Kunth, D., Rodrigues Lacerda, R., & Joguet, B. 2004, MNRAS, 355, 273

Cid Fernandes, R., González Delgado, R. M., Storchi-Bergmann, T., Martins, L. P., & Schmitt, H. 2005, MNRAS, 356, 270

Davies, R., Genzel, R., Tacconi, L., Mueller Sánchez, F., & Sternberg, A.2c. 2007, The Central Engine of Active Galactic Nuclei, 373, 639

Di Matteo, T., Springel, V., & Hernquist, L. 2005, Nature, 433, 604

Dopita, M. A., et al. 2006, ApJS, 167, 177

Dultzin-Hacyan, D., & Benitez, E. 1994, A&A, 291, 720

Dultzin-Hacyan, D., Krongold, Y., Fuentes-Guridi, I., & Marziani, P. 1999, ApJ, 513, L111

Elitzur, M. 2008, Memorie della Societa Astronomica Italiana, 79, 1124

Ellison, S. L., Patton, D. R., Simard, L., & McConnachie, A. W. 2008, AJ, 135, 1877

Ferrarese, L., & Merritt, D. 2000, ApJ, 539, L9

Fiore, F., et al. 2008, ApJ, 672, 94 bibitem[Gebhardt et al.(2000)]2000ApJ...539L..13G Gebhardt, K., et al. 2000, ApJ, 539, L13

Gu, Q., Maiolino, R., & Dultzin-Hacyan, D. 2001, A&A, 366, 765

Ho, L. C., Filippenko, A. V., & Sargent, W. L. W. 1997, ApJS, 112, 315

Hopkins, P. F., & Elvis, M. 2009, arXiv:0904.0649

Hunt, L. K., Malkan, M. A., Salvati, M., Mandolesi, N., Palazzi, E., & Wade, R. 1997, ApJS, 108, 229

Kauffmann, G., et al. 2003a, MNRAS, 346, 1055

Kaviraj, S., et al. 2008, MNRAS, 388, 67

Kawakatu, N., Anabuki, N., Nagao, T., Umemura, M., & Nakagawa, T. 2006, ApJ, 637, 104

Kewley, L. J., Heisler, C. A., Dopita, M. A., & Lumsden, S. 2001, ApJS, 132, 37

Kewley, L.J., Geller, M.J., Barton, E.J., 2006a, AJ, 131,2004

Kewley, L.J., Groves, B. Kauffmann, G., Heckman, T., 2006b, MNRAS, 372, 961

Khalatyan, A., Cattaneo, A., Schramm, M., Gottlöber, S., Steinmetz, M., & Wisotzki, L. 2008, MNRAS, 387, 13

King, A. 2003, ApJ, 596, L27

Knapen, J. H., Shlosman, I., & Peletier, R. F. 2000, ApJ, 529, 93

Knapen, J. H., & James, P. A. 2009, ApJ, 698, 1437

Koulouridis, E., Plionis, M., Chavushyan, V., Dultzin-Hacyan, D., Krongold, Y., & Goudis, C. 2006a, ApJ, 639, 37

Koulouridis, E., Chavushyan, V., Plionis, M., Krongold, Y., & Dultzin-Hacyan, D. 2006b, ApJ, 651, 93

Krongold, Y., Dultzin-Hacyan, D., & Marziani, P. 2002, ApJ, 572, 169

Krongold, Y., Nicastro, F., Brickhouse, N. S., Elvis, M., Liedahl, D. A., & Mathur, S. 2003, ApJ, 597, 832

Krongold, Y., Nicastro, F., Elvis, M., Brickhouse, N., Binette, L., Mathur, S., & Jiménez-Bailón, E. 2007, ApJ, 659, 1022

Krongold, Y., et al. 2009, ApJ, 690, 773

Li, C., Kauffmann, G., Heckman, T. M., White, S. D. M., & Jing, Y. P. 2008, MNRAS, 385, 1915

Lynden-Bell, D. 1969, Nature, 223, 690

Maiolino, R., & Rieke, G. H. 1995, ApJ, 454, 95

Maiolino, R., Ruiz, M., Rieke, G. H., & Papadopoulos, P. 1997, ApJ, 485, 552

Maiolino, R. 2008, New Astronomy Review, 52, 339

Marquez, I., & Moles, M. 1994, AJ, 108, 90

Moles, M., Marquez, I., & Perez, E. 1995, ApJ, 438, 604

Martínez, M. A., Del Olmo, A., Coziol, R., & Perea, J. 2008, Revista Mexicana de Astronomia y Astrofisica Conference Series, 32, 164

Müller Sánchez, F., Davies, R. I., Genzel, R., Tacconi, L. J., Hicks, E., & Friedrich, S. 2008, Revista Mexicana de Astronomia y Astrofisica Conference Series, 32, 109

Murray, N., Quataert, E., & Thompson, T. A. 2005, ApJ, 618, 569

Nelson, C. H., & Whittle, M. 1996, ApJ, 465, 96

Nicastro, F. 2000, ApJ, 530, L65

Shu, X.-W., Wang, J.-X., & Jiang, P. 2008, Chinese Journal of Astronomy and Astrophysics, 8, 204

Silk, J., & Rees, M. J. 1998, A&A, 331, L1

Springel, V., Di Matteo, T., & Hernquist, L. 2005, ApJ, 620, L79

Stasińska, G., Cid Fernandes, R., Mateus, A., Sodré, L., & Asari, N. V. 2006, MNRAS, 371, 972

Stocke, J.T., et al. 1991, ApJS, 76, 813

Storchi-Bergmann, T., González Delgado, R. M., Schmitt, H. R., Cid Fernandes, R., & Heckman, T. 2001, ApJ, 559, 147

Tang, Y.-W., Kuo, C.-Y., Lim, J., & Ho, P. T. P. 2008, ApJ, 679, 1094

Tran, H. D. 2003, ApJ, 583, 632

Umemura, M., Fukue, J., & Mineshige, S. 1998, MNRAS, 299, 1123

Veilleux, S., & Osterbrock, D. E. 1987, ApJS, 63, 295

Wake, D. A., et al. 2004, ApJ, 610, L85

Wang, L., & Kauffmann, G. 2008, arXiv:0801.3530

Watson, M.G., et al. 2009, A&A, 493, 339

Table 1. The sample of Sy1 galaxies in our spectroscopic survey. Below each AGN we list all its neighbours within a projected distance of 100 h^{-1} kpcs.

NAME	RA J2000.0	DEC J2000.0	$O_{\rm MAPS}$ integrated	z
NGC 863	02 14 33.5	−00 46 00	14.58	0.0270
neighbour 1	02 14 29.3	−00 46 05	18.25	0.0270
MRK 1400	02 20 13.7	+08 12 20	17.07	0.0293
neighbour 1	02 19 59.8	+08 10 45	17.25	0.0284
NGC 1019	02 38 27.4	+01 54 28	15.02	0.0242
neighbour 2	02 38 25.4	+01 58 07	16.28	0.0203
NGC 1194	03 03 49.1	−01 06 13	15.38	0.0134
neighbour 1	03 03 41.2	−01 04 25	16.99	0.0140
neighbour 4	03 04 12.5	−01 11 34	15.75	0.0130
1H 1142−178	11 45 40.4	−18 27 16	16.82	0.0329
neighbour 1	11 45 40.9	−18 27 36	18.01	0.0322
neighbour 2	11 45 38.8	−18 29 19	18.45	0.0333
MRK 699	16 23 45.8	+41 04 57	17.21	0.0342
neighbour 1	16 23 40.4	+41 06 16	17.59	0.0334
NGC 7469	23 03 15.5	+08 52 26	14.48	0.0162
neighbour 1	23 03 18.0	+08 53 37	15.58	0.0156
NGC 526A*	01 23 54.5	−35 03 56	15.69†	0.0191
neighbour 1	01 23 57.1	−35 04 09	15.80†	0.0188
neighbour 2	01 23 58.1	−35 06 54	15.68†	0.0189
neighbour 3	01 24 09.5	−35 05 42	16.37†	0.0185
neighbour 4	01 23 59.2	−35 07 38	16.04†	0.0185
NGC 5548	14 17 59.5	+25 08 12	14.18	0.0172
neighbour 1	14 17 33.9	+25 06 52	17.16	0.0172
NGC 6104	16 16 30.7	+35 42 29	15.11	0.0279
neighbour 1	16 16 49.9	+35 42 07	16.44	0.0264

†Calculated from $O_{\rm USNO}$, using relation $O_{\rm MAPS} = 14.61(\pm1.25) + 0.11(\pm0.11)O_{\rm USNO}$ using Véron-Cetty et al. (2004) Table 2.

*Region Not Covered by MAPS Catalog

Table 2. The sample of Sy2 galaxies in our spectroscopic survey. Below each AGN we list all its neighbours within a projected distance of 100 h^{-1} kpc.

NAME	RA J2000.0	DEC J2000.0	$O_{\rm MAPS}$ integrated	z
ESO 545-G013	02 24 40.5	−19 08 31	14.41	0.0338
neighbour 1	02 24 50.9	−19 08 03	16.19	0.0340
NGC 3786	11 39 42.5	+31 54 33	13.88	0.0091
neighbour 1	11 39 44.6	+31 55 52	13.53	0.0085
UGC 12138	22 40 17.0	+08 03 14	15.93	0.0250
neighbour 1	22 40 11.0	+07 59 59	18.77	0.0236
UGC 7064	12 04 43.3	+31 10 38	15.11	0.0250
neighbour 1(2)⋆	12 04 45.6	+31 11 27	16.68	0.0236
neighbour 1	12 04 45.2	+31 11 33	16.33	0.0244
neighbour 2	12 04 45.1	+31 09 34	16.33	0.0261
IRAS 00160−0719	00 18 35.9	−07 02 56	15.73	0.0187
neighbour 1	00 18 33.3	−06 58 54	17.80	0.0173
ESO 417-G06	02 56 21.5	−32 11 08	15.54	0.0163
neighbour 1	02 56 40.5	−32 11 04	17.43	0.0163
NGC 1241	03 11 14.6	−08 55 20	13.56	0.0135
neighbour 1	03 11 19.3	−08 54 09	15.41	0.0125
NGC 1320	03 24 48.7	−03 02 32	14.59	0.0090
neighbour 1	03 24 48.6	−03 00 56	15.07	0.0095
MRK 612	03 30 40.9	−03 08 16	15.78	0.0207
neighbour 1	03 30 42.3	−03 09 49	16.13	0.0205
NGC 1358	03 33 39.7	−05 05 22	13.98	0.0134
neighbour 2	03 33 23.5	−04 59 55	14.95	0.0131
IC 4553	15 34 57.1	+23 30 16	14.43	0.0181
neighbour 1	15 34 57.3	+23 30 05	15.68	0.0190
NGC 7672	23 27 31.4	+12 23 07	15.23	0.0134
neighbour 1	23 27 19.3	+12 28 03	14.67	0.0138
NGC 7682	23 29 03.9	+03 32 00	14.88	0.0171
neighbour 1	23 28 46.6	+03 30 41	14.64	0.0171
NGC 7743	23 44 21.1	+09 56 03	12.16	0.0044
neighbour 3	23 44 05.5	+10 03 26	16.95	0.0054

*this galaxy is merging with neighbour 1 and was not resolved in koulouridis et al. 2006a.

Table 3. The sample of BIRG galaxies in our spectroscopic survey. Below each BIRG we list all its neighbours within a projected distance of 100 h^{-1} kpc with their measured redshifts.

NAME	RA J2000	DEC J2000	$O_{\rm MAPS}$ integrated	z
UGC00556	00 54 50.3	29 14 48	15.63	0.0154
neighbour 1	00 54 51.1	29 16 25	17.03	0.0154
NGC0835	02 09 24.6	−10 08 09	13.67⋆	0.0138
neighbour 1	02 09 20.8	−10 07 59	⋆	0.0129
neighbour 2	02 09 38.6	−10 08 46	14.89	0.0129
neighbour 3	02 09 42.9	−10 11 03	15.01	0.0131
NGC0877	02 17 59.6	14 32 39	13.07	0.0131
neighbour 1	02 17 53.3	14 31 17	16.04	0.0129
neighbour 2	02 17 26.3	14 34 49	16.77	0.0134
NGC0922	02 25 04.4	−24 47 17	13.25	0.0103
neighbour 1	02 24 30.0	−24 44 44	16.73	0.0105
NGC0992	02 37 25.5	21 06 03	15.39	0.0138
neighbour 1	02 37 28.2	21 08 31	16.99	0.0136
NGC1614	04 33 59.8	−08 34 44	14.55	0.0160
neighbour 1	04 34 00.3	−08 34 46	16.44	0.0159
NGC2785	09 15 15.4	40 55 03	14.85	0.0088
neighbour 2	09 14 43.1	40 52 47	14.54	0.0083
neighbour 3	09 14 35.6	40 55 24	17.58	0.0089
NGC2856	09 24 16.0	49 14 57	14.71	0.0088
neighbour 1	09 24 03.1	49 12 15	14.52	0.0092
NGC3221	10 22 20.0	21 34 10	13.87	0.0137
neighbour 1	10 22 26.0	21 32 31	17.06	0.0117
neighbour 2	10 22 21.1	21 31 00	17.89	0.0128
NGC3690	11 28 31.0	58 33 41	13.76⋆	0.0104
neighbour 1	11 28 33.5	58 33 47	⋆	0.0104
neighbour 2	11 28 27.3	58 34 42	⋆	0.0132
NGC5433	14 02 36.1	32 30 38	14.68	0.0145
neighbour 1	14 02 38.9	32 27 50	18.00	0.0148
neighbour 2	14 02 20.5	32 26 53	16.17	0.0141
NGC5990	15 46 16.3	02 24 56	14.29	0.0128
neighbour 3	15 45 45.9	02 24 35	15.87	0.0135

Table 3—Continued

NAME	RA J2000	DEC J2000	$O_{\rm MAPS}$ integrated	z
NGC7541	23 14 43.9	04 32 04	13.22	0.0089
neighbour 1	23 14 34.5	04 29 54	14.70	0.0089
NGC7714*	23 36 14.1	02 09 19	13.10†	0.0093
neighbour* 1	23 36 22.1	02 09 24	14.90†	0.0092
NGC7771	23 51 24.9	20 06 43	13.81⋆	0.0143
neighbour 1	23 51 22.5	20 05 47	⋆	0.0143
neighbour 2	23 51 13.1	20 06 12	17.13	0.0137
neighbour 3	23 51 04.0	20 09 02	14.05	0.0140

†Zwicky blue magnitude (Region Not Covered by MAPS Catalog)

⋆Not resolved neighbouring galaxies

Table 4. Emission line ratios and classification.

NAME	$[OIII]/H\beta$)	$([NII]/H\alpha)$	$([SII]/H\alpha)$	Stasińska	BPT
Sy1 galaxies					
NGC 863					
neighbour 1	-	-	-	normal	normal
MRK 1400					
neighbour 1	0.57±0.05	0.32±0.01	0.36±0.02	SB	SB
NGC 1019					
neighbour 2	0.58±0.13	0.50±0.01	0.45±0.02	TO	TO
NGC 1194					
neighbour 1	0.37±0.03	0.33±0.01	0.36±0.01	SB	SB
neighbour 4	0.40±0.06	0.39±0.01	0.39±0.02	SB	SB
1H 1142−178					
neighbour 1	-	-	-	normal	normal
neighbour 2	-	0.44±0.07	0.79±0.10	TO	-
MRK 699					
neighbour 1	-	0.70±0.06	0.56±0.05	TO	-
NGC 7469					
neighbour 1	0.43±0.05	0.39±0.01	0.29±0.01	SB	SB
NGC 526A					
neighbour 1*	-	1.37±0.22	0.79±0.19	AGN	-
neighbour 2	-	-	-	normal	normal
neighbour 3	0.32±0.10	0.35±0.02	0.42±0.04	SB	SB
neighbour 4	0.57±0.08	0.35±0.01	0.40±0.07	SB	SB
NGC 5548					
neighbour 1	0.60±0.12	0.42±0.01	0.57±0.01	TO	SB
NGC 6104					
neighbour 1	-	-	-	normal	normal
Sy2 galaxies					
ESO 545-G013					

Table 4—Continued

NAME	$[OIII]/H\beta$)	$([NII]/H\alpha)$	$([SII]/H\alpha)$	Stasińska	BPT
neighbour 1	-	0.40±0.03	0.39±0.05	SB	-
NGC 3786					
neighbour 1†	-	1.19±0.12	0.95±0.12	AGN	-
UGC 12138					
neighbour 1	4.16±0.39	0.06±0.01	0.18±0.01	SB	SB
UGC 7064					
neighbour 1(2)	0.50±0.13	0.42±0.03	0.17±0.03	TO	SB
neighbour 1†	-	4.2±0.5	2.4±0.3	AGN	-
neighbour 2	0.41±0.06	0.46±0.01	0.44±0.01	TO	SB
IRAS 00160−0719					
neighbour 1	0.97±0.07	0.25±0.01	0.44±0.03	SB	SB
ESO 417-G06					
neighbour 1	1.16±0.14	0.21±0.01	0.29±0.02	SB	SB
NGC 1241					
neighbour 1	1.35±0.25	0.37±0.01	0.37±0.02	SB	TO
NGC 1320					
neighbour 1	-	-	-	normal	normal
MRK 612					
neighbour 1	-	-	-	normal	normal
NGC 1358					
neighbour 2	-	-	-	normal	normal
IC 4553					
neighbour 1				merger	
NGC 7672					
neighbour 1	-	-	-	normal	normal
NGC 7682					
neighbour 1	1.56±0.11	0.45±0.01	0.29±0.01	TO	TO
NGC 7743					
neighbour 3	2.50±0.17	0.07±0.01	0.25±0.01	SB	SB

BIRGs

Table 4—Continued

NAME	$[OIII]/H\beta$)	$([NII]/H\alpha)$	$([SII]/H\alpha)$	Stasińska	BPT
UGC00556					
neighbour 1	0.78±0.04	0.25±0.01	0.33±0.01	SB	SB
NGC0835					
neighbour 1*	-	1.85±0.07	1.56±0.12	AGN	-
neighbour 2	0.36±0.01	0.38±0.01	0.24±0.001	SB	SB
neighbour 3	1.73±0.31	0.62±0.01	0.41±0.01	TO	TO
NGC0877					
neighbour 1	-	0.68±0.06	0.54±0.09	TO	-
NGC0922					
neighbour 1	7.86±0.82	0.08±0.01	0.13±0.01	SB	SB
NGC0992					
neighbour 1	3.64±0.09	$0.12\pm < 0.005$	0.17±0.01	SB	SB
NGC1614					
neighbour 1				merger	
NGC2785					
neighbour 2	0.85±0.12	0.25±0.01	0.37±0.02	SB	SB
neighbour 3	1.81±0.17	0.10±0.01	0.25±0.02	SB	SB
NGC2856					
neighbour 1	-	0.60±0.02	0.45±0.02	TO	-
NGC3221					
neighbour 1	-	-	-	normal	normal
neighbour 2	-	-	-	normal	normal
NGC3690					
neighbour 1	1.48±0.19	0.41±0.01	0.28±0.02	TO	TO
neighbour 2	-	-	-	normal	normal
NGC5433					
neighbour 1	1.87±0.14	0.16±0.01	0.33±0.01	SB	SB
neighbour 2	-	0.97±0.05	0.50±0.04	AGN	-
NGC5990					
neighbour 3	0.41±0.02	$0.36\pm < 0.005$	$0.25\pm < 0.005$	SB	SB

Table 4—Continued

NAME	$[OIII]/H\beta$)	$([NII]/H\alpha)$	$([SII]/H\alpha)$	Stasińska	BPT
NGC7541					
neighbour 1	-	0.62±0.02	0.40±0.02	TO	
NGC7714					
neighbour 1	-	-	-	normal	normal
NGC7771					
neighbour 1	0.74±0.03	0.40±0.01	0.34±0.01	SB	SB
neighbour 2	3.9±1.2	0.11±0.03	0.35±0.03	SB	SB
neighbour 3	0.42±0.08	0.61±0.01	0.29±0.01	TO	TO

†Bad spectrum. Ambiguous classification.

⋆The spectrum is bad but we can clearly see a profound [OI] emission line, based on which we classify as AGN.

Table 5. XMM observations

Name	2XMM ID	Opt. Class	$logL_X$ (0.5-8 keV) erg s^{-1}	Flux (0.5-8 keV) erg cm^{-2} s^{-1}	X/O offset arcmin	HR
NGC1194-N1	-	SB	< 39.59	$< 7.3 \times 10^{-15}$	-	-
NGC1194-N4	-	SB	< 39.72	$< 1.1 \times 10^{-14}$	-	-
NGC526A-N1	J012357.0-350410	AGN	40.46	3.3×10^{-14}	0.023	-0.28 ± 0.09
NGC526A-N2	J012358.1-350653	Normal	40.75	5.9×10^{-14}	0.008	0.05 ± 0.1
NGC526A-N3	-	SB	<39.65	$< 4.7 \times 10^{-15}$	-	-
NGC526A-N4	J012359.0-350741	SB	39.95	9.4×10^{-15}	0.035	-0.61 ± 0.29
UGC12138-N1	-	SB	<40.63	$< 2.8 \times 10^{-14}$	-	-
NGC1320-N1	J032448.6-030057	Normal	39.46	1.2×10^{-14}	0.020	-0.38 ± 0.17
MRK612-N1	J033042.5-030949	Normal	39.59	3.4×10^{-15}	0.060	-0.67 ± 0.24
NGC1358-N2	J033323.3-045953	Normal	40.19	3.8×10^{-14}	0.044	0.05 ± 0.3
NGC7682-N1	J232846.7+033041	TO	42.04	1.30×10^{-12}	0.026	-0.32 ± 0.02
NGC7743-N1	J234427.4+095308	Normal	39.54	5.9×10^{-14}	0.023	-0.93 ± 0.13
NGC7743-N3	-	SB	<39.44	3.4×10^{-14}	-	-
NGC3786-N1	J113944.3+315547	AGN	39.7326	2.7×10^{-14}	0.08	-0.46 ± 0.30

Table 6. The size/magnitude and activity type of neighbours of Seyfert galaxies as a function of their relative separation.

type/distance	10	20	30	40	50	60	70	80	90	100
Normal	L	**VL**	S **VL**			VL	**VL**	**L**		L
SB		L		S	**S**	**S**	S S **S**	**S**	S VL **S**	VL
TO		**S**				VL	**VL**	L		
AGN	VL **M**	**VL**								

[1]With bold fonts we mark the neighbours of Sy2 galaxies

Spectra of the neighbours of AGN or BIRG galaxies, listed in Tables 1, 2 & 3.

MRK1400 1

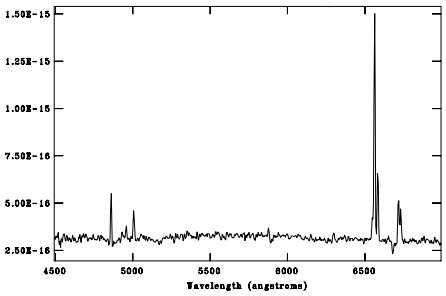

NGC1019 2

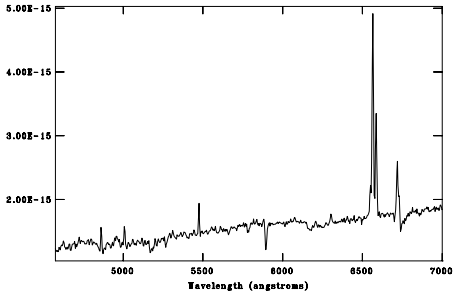

NGC1194 1 (SDSS)

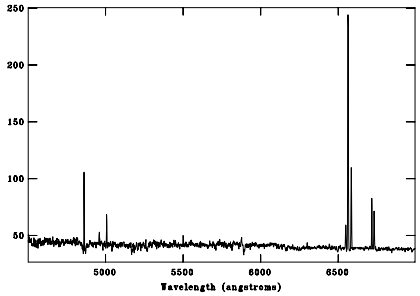

NGC1194 4

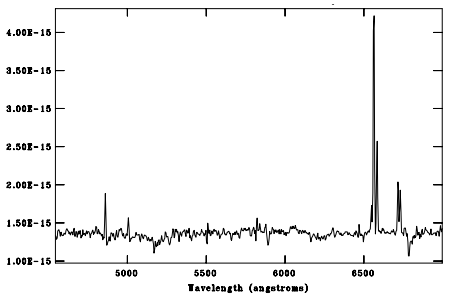

1H1142 2

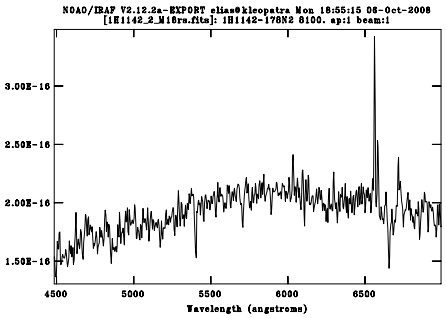

MRK699 1

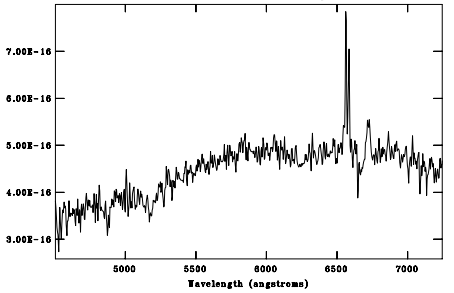

NGC7469 1

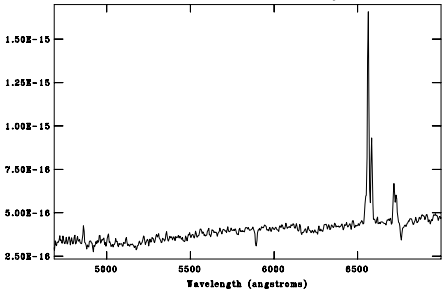

NGC526a 1

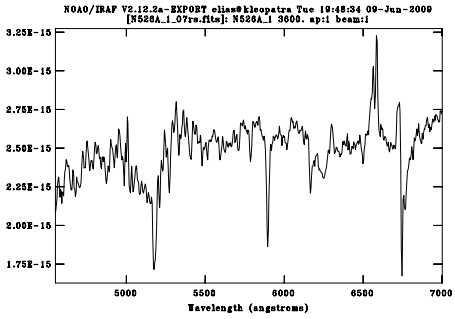

NGC526a 3

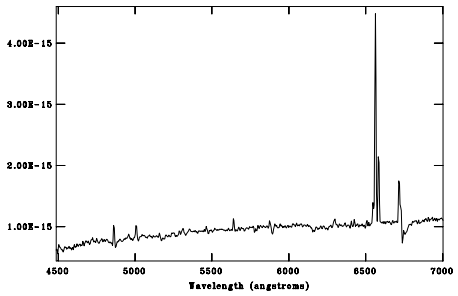

NGC526a 4

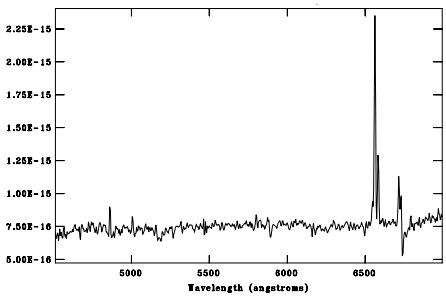

NGC5548 (SDSS) 1

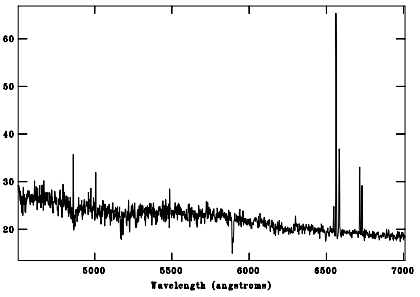

ESO545-G013 1

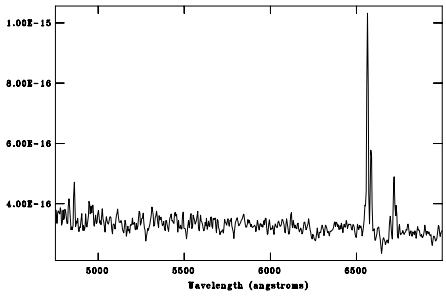

NGC3786 1

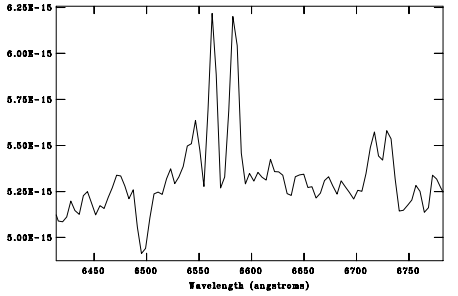

UGC12138 1

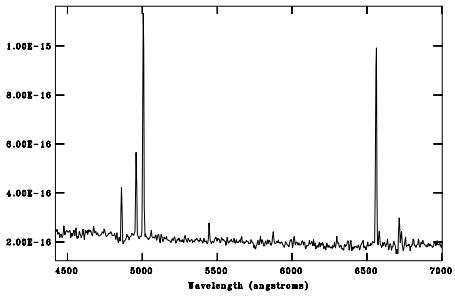

UGC7064 1 (2)

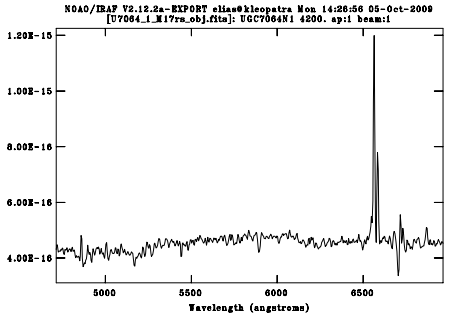

UGC7064 1 (SDSS)

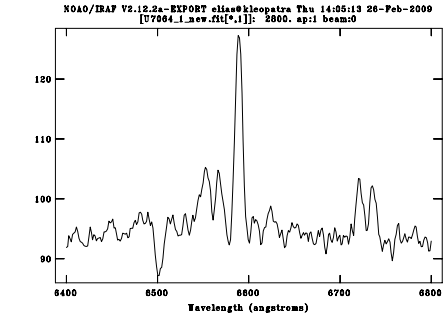

UGC7064 2

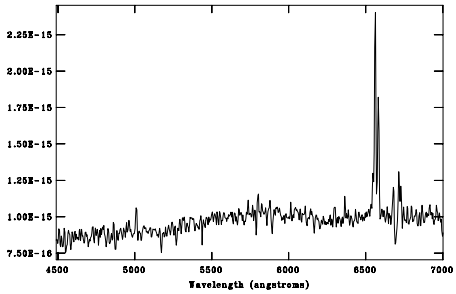

IRAS00160-0719 1

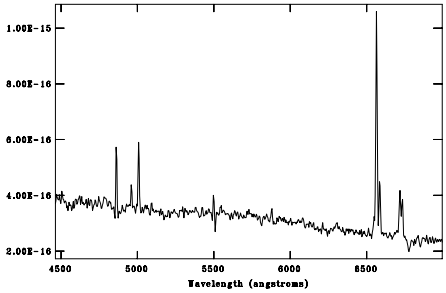

ESO417-G06 1

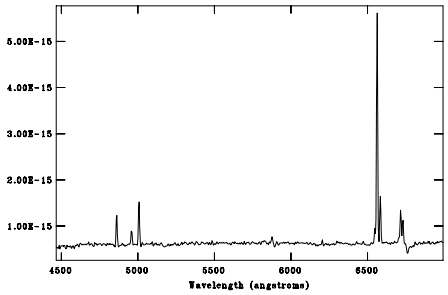

NGC1241 1 1

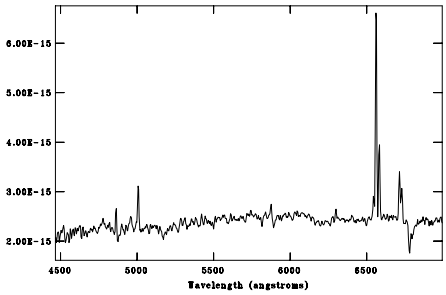

IC4553 1

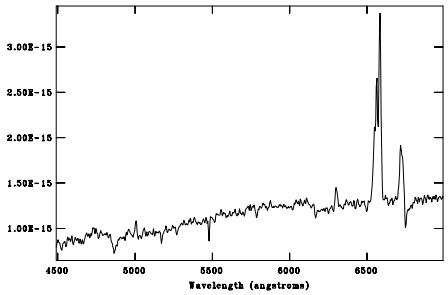

NGC7682 1

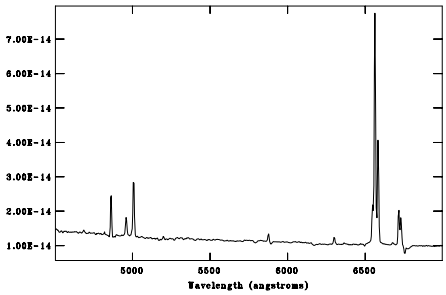

NGC7743 3

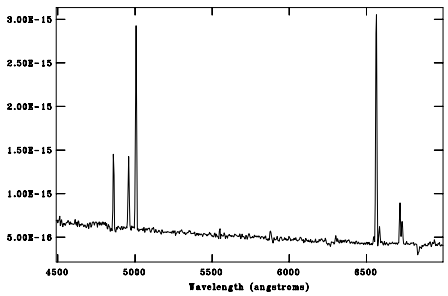

UGC00556 1

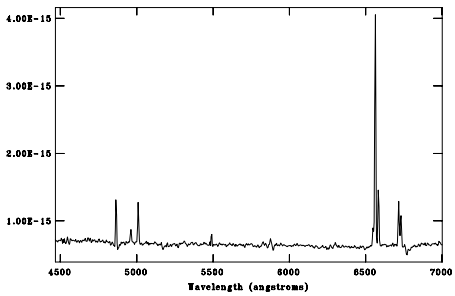

14h02m20.5s +32d26m53s NGC835 1

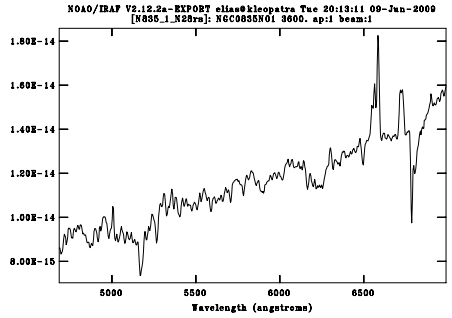

NGC835 2 (SDSS)

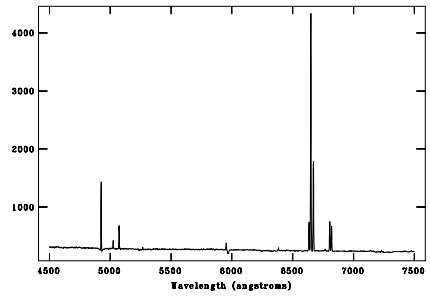

NGC835 3

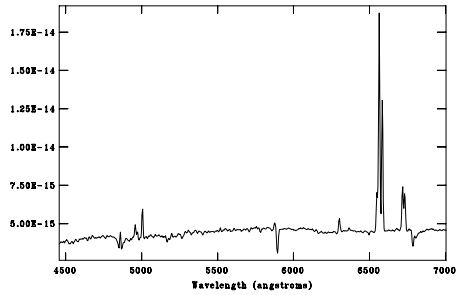

NGC877 1

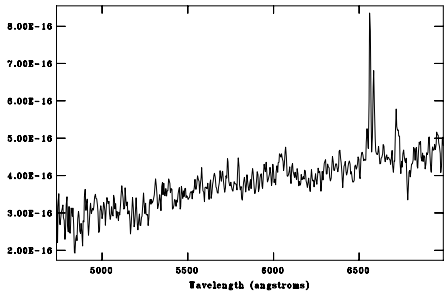

NGC922 1

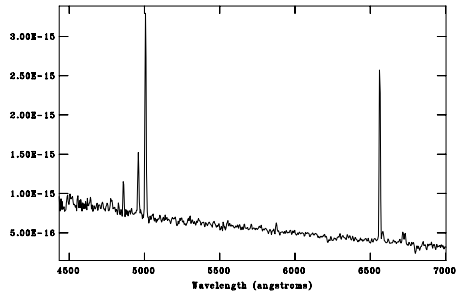

NGC992 1

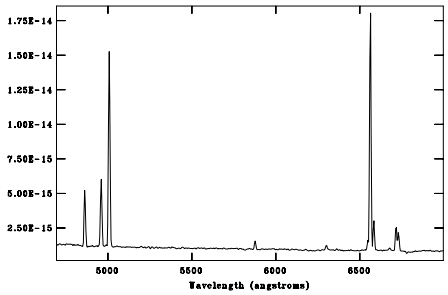

NGC2785 2

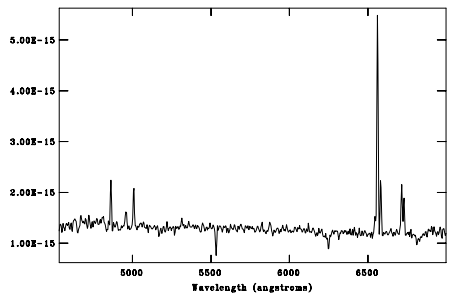

NGC2785 3

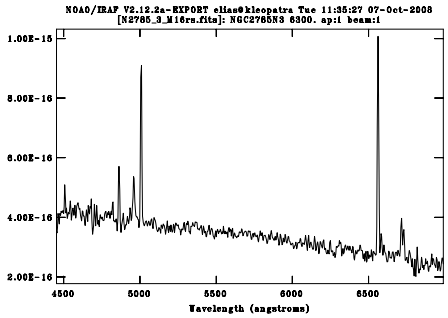

NGC2856 1

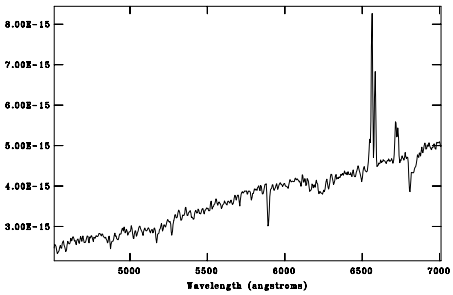

NGC3690 1 (SDSS)

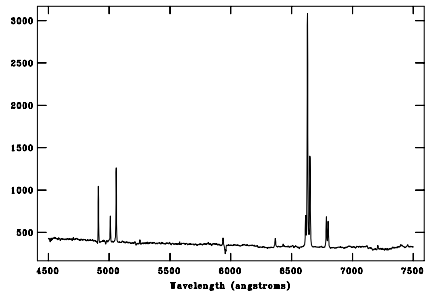

NGC5433 1

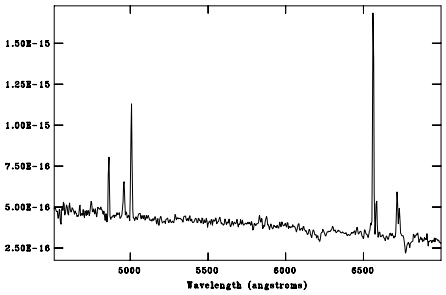

NGC5433 2

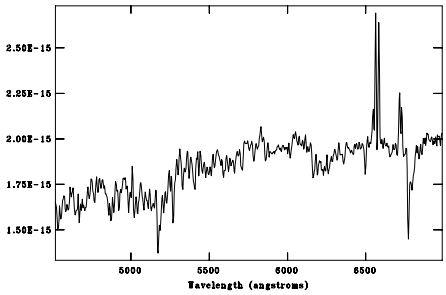

NGC5990 3 (SDSS)

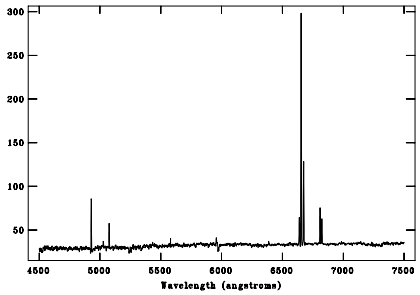

NGC7541 1

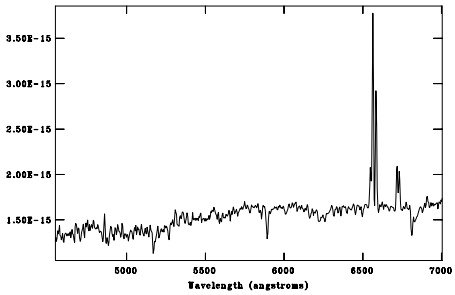

NGC7771 1

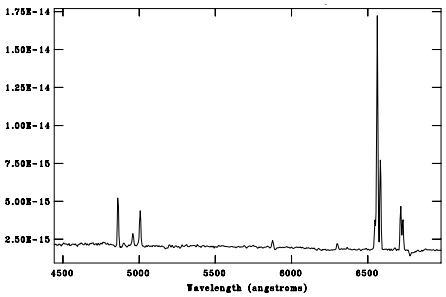

NGC7771 2

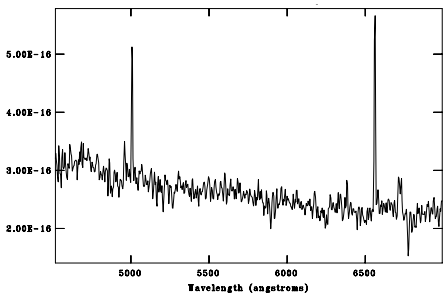

NGC7771 3

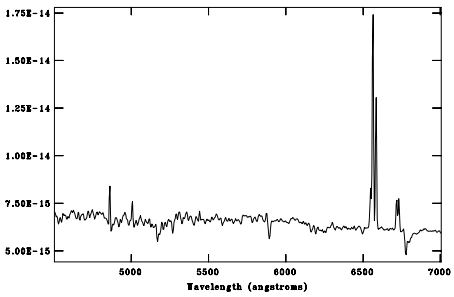
1.75E-14
1.50E-14
1.25E-14
1.00E-14
7.50E-15
5.00E-15
5000
5500
6000
6500
7000
Wavelength (angstroms)